PCCP

Accepted Manuscript

ROYAL SOCIETY OF CHEMISTRY

www.rsc.org/pccp

Enhancement of T_c in atomic phase of iodine-doped hydrogen at high pressures

Defang Duan, Fubo Tian, Yunxian Liu, Xiaoli Huang, Da Li, Hongyu Yu, Yanbin Ma, Bingbing Liu, Tian Cui[*]

State Key Laboratory of Superhard Materials, College of Physics, Jilin University, Changchun, 130012, P. R. China

ABSTRACT: The high-pressure structures and superconductivity of iodine-doped hydrogen have been studied by *ab initio* calculations. Above 100 GPa, we discover a stable phase with *Pnma* symmetry in the H_2I stoichiometry that consist of monatomic iodine tube trapping hydrogen molecule units. Interestingly, H_2 molecule units dissociate and form a novel atomic phase with *R*-3*m* symmetry at 246 GPa. Further electron-phonon coupling calculations predict critical temperature of superconductivity T_c to be 3.8 K for *Pnma* phase and 33 K for *R*-3*m* phase at 240 GPa. Significantly, the T_c of *R*-3*m* phase is enhancement approximately 8 times than that of *Pnma* phase, which is mainly attributed to H_2 molecules are broken exhibiting a atomic character in *R*-3*m* phase.

Keywords: atomic phase, superconductivity, high-pressure, *ab initio* calculations, hydrogen-iodine system

INTRODUCTION

Back in the year 1935, Wigner and Huntington proposed that molecular hydrogen would dissociate into an atomic phase with metallic properties at high pressures[1]. Over thirty years later, Ashcroft (1968) predicted that the atomic metallic hydrogen would be a room-temperature superconductor[2]. Ever since this prediction, the high pressure structures, metallization and superconductivity of hydrogen have been extensively studied and the steps will never stop. Following more recent advancements in structure prediction methods, a atomic phase with $I4_1/amd$ symmetry similar to the phase IV of cesium is found[3]. This structure is stable above 490 GPa with critical temperature T_c of 365 K[4, 5]. Unfortunately, the metallization of solid hydrogen has still not been observed up to 360 GPa in experiment[6, 7]. One of the important topics is how to reduce the metallic pressure of hydrogen system. In 2004, Aschroft[8] suggested that hydrogen-dominated compounds can metallize at much lower pressures than pure hydrogen, and may be potential high temperature superconductors. In these systems, other components can be viewed as "impurities", and the hydrogen is chemically precompressed by “impurities”.

From then on, a large number of efforts have focused on searching for the likely high-temperature superconductors in hydrogen-rich materials. Theoretical investigations revealed that the group IVA hydrides present high temperature superconductivity at high pressures, e.g. 16~75 K for SiH_4[9, 10], 64 K for GeH_4,[11] 62~80 K for SnH_4 [12, 13], 139 K for Si_2H_6 [14]. Besides the naturally existed hydrides, more attentions are paid to the new hydrogen-rich compounds appear at high pressures. **N**ew H_2-containing van der Waals compounds $SiH_4(H_2)_2$[15] and $GeH_4(H_2)_2$[16] were predicted to be superconductors with high T_c values of 107 K and 90 K at 250 GPa, respectively. Superconductivity was also reported in another new metal hydride LiH_6[17], KH_6[18], and CaH_6[19], where T_c reach 65 K at 160 GPa, 82 K at 300 GPa, and 235 K at 150 GPa, respectively. Recently,

the novel sulfur hydrides H_3S[20, 21] was predicted theoretically to be a high-temperature superconductor with T_c reaching as high as 191 ~ 204 K at 200 GPa, which has been approved by the subsequent high-pressure experiment,[22] yielding a research hotspot in condensed matter physics and material science.

Iodine hydrides can be an interesting subject of this study. The only known iodine hydride is HI with a complex triclinic *P*-1 structure at low temperature and ambient pressure[23]. At high pressure, HI undergoes three transition by experiment measurements: an insulator to metal transition, a molecular to atomic phase transition, and an additional transition in which I_2, I^{3-} complex and alloy of metallic hydrogen $H_{2-x}I_x$ would be appear[24, 25]. After that HI is seldom to be studied under high pressure.

What happened to HI at high pressures? Whether the H-rich hydrogen-iodine compounds are stable and have high T_c at high pressures. To answer these questions, we study the high-pressure stability of different stoichiometric HI_3, HI_2, and H_nI (n=1-6) and further explore their superconductivity by *ab initio* calculations. Results show that HI is unstable, while three new energetically stable stoichiometries (H_2I, H_4I, and H_5I) are uncovered at high pressure. More recently, A. Shamp and E. Zurek predicted the crystal structures and superconductivity of iodine polyhydrides below 200 GPa.[26] They also found stoichiometries H_2I, H_4I, and H_5I, and estimated T_c of H_2I and H_4I to be 7.8 and 17.5 K at 100 GPa, respectively. In the present work, we found a metallic atomic phase with *R*-3*m* symmetry in H_2I at 246 GPa, which is approximately one-half of the currently suggested pressure of atomic metallic hydrogen. Moreover, the T_c of atomic phase is estimated to be 33 K at 240 GPa which is improved nearly 8 times than that of H_2I-*Pnma* phase containing qusia-H_2 molecules.

COMPUTATIONAL METHOD

To obtain stable structures for hydrogen-iodine system, we conducted structure prediction based on the particle swarm optimization algorithm as implemented in CALYPSO[27, 28]. The underlying structure relaxations were performed using the projector augmented waves (PAW) method[29], as implemented in the Vienna *ab initio* simulation package VASP code[30]. The electron-ion interaction was described by the PAW potentials taken from the VASP library with $1s^1$ and $5s^25p^5$ as valence electrons for H and I atoms, respectively. The generalized gradient approximation of Perdew-Burke-Ernzerhof[31] was used to describe the exchange-correlation potential. The energy cutoff of 500 eV and k-mesh of $2\pi\times0.03$ Å^{-1} within the Monkhorst-Pack scheme were chosen to ensure that the total energy is well converged to better than 1 meV/atom. Lattice dynamics and electron-phonon coupling have been computed with QUANTUM-ESPRESSO[32]. The plane-wave pseudopotential method with norm-conserving potentials were used. Convergence tests gave a suitable value of 80 Ry kinetic energy cutoff. The q-point mesh in the first BZ of 5×5×3 for H_2I-*R*-3*m*, 3×5×3 for H_2I-*Pnma* and 7×7×7 for H_4I-*P*6/*mmm* structures were used in the interpolation of the force constants for the phonon dispersion curve calculations. A denser k-point mesh 20×20×12 for H_2I-*R*-3*m*, 20×20×12 for H_2I-*Pnma* and 28×28×28 for H_4I-*P*6/*mmm* structures were adopted. The hybrid functional HSE06[33, 34] was used to calculate the band gaps of H_5I-$P222_1$ structure, together with a cutoff energy of 720 eV and norm-conserving pseudopotentials, implemented in the CASTEP code[35].

RESULTS AND DISCUSSION

The variable-cell structure prediction simulations are performed with considering the unit cells sizes from 1 to 4 formula units (f.u.) for HI_3, HI_2, H_nI (n=2-6), and 1 to 8 f.u. for HI between 10

and 300 GPa. The calculated formation enthalpies of identified ground state structures for H-I system at 50, 100, 150, 200, 250 and 300 GPa are provided in Fig. 1. The reference level is hydrogen and iodine in their most stable forms at the pressure specified.[3, 36-38] The convex hull is plotted in solid line and connects the thermodynamically stable compositions, which can be synthesized experimentally in principle. At 50 GPa, H_5I is the only stable composition, as shown in Fig. 1. When the pressure increases to 100 GPa, a new composition H_2I occurs. At 150 GPa, both of H_2I and H_4I emerge on the convex hull, while H_5I is already unstable and decomposes into H_4I and H_2. Moreover, H_2I and H_4I are remain stable up to 300 GPa, and H_2I is the global minimum compound above 150 GPa. It is noted that HI is absent on the convex hell because it decomposes into solids H_2 and I_2 at about 6.7 GPa, as shown in Fig. S1. In addition, HI_3, HI_2, and H_6I are also absent on the convex hull, indicating they are unstable in the whole pressure range. The zero-point energy (ZPE) is not included in the calculation of the formation enthalpies of H-I system (Fig. 1a). To investigate the vibrational effects on the phase stability, ZPEs of H_2I, H_4I and H_5I are estimated using the quasi-harmonic approximation at 50, 100, 200 and 300 GPa, as shown in Fig. S2. It is found that the inclusion of ZPEs significantly lowered the formation enthalpies, but the stability of these compounds remains unaltered.

The stable pressure ranges and crystal structures of our predicted three stable compounds (H_2I, H_4I and H_5I) are shown in Fig. 1b and Fig. 2, respectively. H_2I is stable at 100 GPa with space group *Pnma*. In this structure, iodine atoms form a tube network that trap hydrogen molecules units (H-H contact of 0.802 Å) in channels, as depicted in Fig. 2a. The shortest distance of H-I is 2.089 Å at 100 GPa, suggesting the weak interaction between H and I. In addition, the shortest distance of I-I is 2.887 Å, as compared with 2.906 Å in atomic phase of iodine (Fm-3m) at 100 GPa[38]. We have also found a competitive structure with *Cmcm* symmetry, and the enthalpy of

Cmcm is only 10 meV/f.u. higher than that of *Pnma*, as shown in Fig. 3. Since this is a metastable structure, we will not discuss it in the following text. Further compression to 246 GPa, a distinctive structure with *R*-3*m* symmetry occurs, in which iodine atoms and hydrogen atoms form puckered 2D nets with edge-shard H_6I units, as shown in Fig. 2b. Strikingly, the shortest H-H distance at 260 GPa is 1.10 Å, much longer than intramolecular bond length ~0.756 Å in molecular phase (*Cmca*) of solid H_2, and close to the H-H bond length ~1.05 Å in atomic phase (*I*4/*amd*) of solid H_2 at this pressure. The longer H-H bond length indicates that they are in the form of atomic phase other than molecular phase.

In addition, to understand the molecular interactions, the nearest intramolecular and intermolecular bond distances of H_2I as functions of pressure are depicted in Fig. 3b. The intermolecular bond lengths of H1-H2, H1-I1 and I1-I2 decrease with increasing pressure, while the intramolecular bond length of H1-H1 increases in the *Pnma* phase. It is indicating that the strength of H-I interaction with increasing pressure elongates intramoleulcar covalent bonds for H_2 molecular units. Then, the H_2 molecules dissociated to hydrogen atoms at about 250 GPa, and the structure is reconstructive with *R*-3*m* symmetry. It is also noted that the bond length of H1-I1 and I1-I2 are continuation, whereas the bond length of H-H change abruptly at the phase transition pressure.

To further understand the bonding nature of the *Pnma* and *R*-3*m* phases, we calculated the electron localization function (ELF), as depicted in Fig. 4. High ELF values indicate paired electrons, i.e., lone pairs (close 1.0) and covalent bonds (>0.75), whereas values around 0.5 indicate a uniform electron gas. Not surprisingly, the highest ELF values are found in the region of H and I lone pairs. In the *Pnma* phase, one can see ELF values of 0.9 between two H atoms within the unit, indicating a strong covalent feature. In the case of *R*-3*m* phase, the value of ELF

between the nearest H-H, H-I, and I-I is about 0.5~0.6, indicating that covalent bond is non-existent, which is more likely a atomic phase with a uniform electron gas.

H_4I is predicted to possess a hexagonal *P*6/*mmm* structure which is stable above 110 GPa, which is the same with A. Shamp and E. Zurek predicted.[26] In this structure, iodine atoms occupy lattice sites forming 1-D chain along the c axis and the H_2 molecular units (H-H contact of 0.803 Å) also parallel to the c axis, as shown in Fig. 2c. For H_5I, it adopts a $P222_1$ symmetry which becomes stable with respect to decomposition into solids H_2 and I_2 at about 20 GPa (Fig. S3a). At 114 GPa, it decomposes into H_4I (*P6/mmm*) and H_2 (Fig. S3b). H_5I-$P222_1$ is consisted of zigzag rectangular chains built from [I–H–I] units and H_2 molecular units, as shown in Fig. 2d. In the rectangular chains, H situates at the middle of two I atoms leading to symmetric hydrogen bonds. Further analysis of ELF shows the moderate values (0.8) between H and I, suggesting covalent bond (Fig. 3). The lattice parameters of these stable structures at different pressures are listed in Table S1 of the supplementary information.

The electronic band structure and band gap for all stable structures at selected pressures are also explored, as depicted in Fig. 5. The H_2I-*Pnma*, H_2I-*R*-3*m*, and H_4I-*P*6/*mmm* are good metals with the band cross the Fermi level. The band structure of H_2I-*Pnma* is analogous to H_4I-*P*6/*mmm*, but different from H_2I-*R*-3*m*, which is due to H atoms arrangement. The band gaps of H_5I-$P222_1$ structure are calculated by performing HSE06 hybrid functional. It is an insulator with an indirect band gap of 2.892 eV at 20 GPa. The band gap for the $P222_1$ structure decreases with increasing pressure and closes at approximately 100 GPa.

To explore the possible superconductivity of H-I system at high pressures, the electron phonon coupling (EPC) λ and logarithmic average phonon frequency ω_{log} are calculated, as shown in

Table SII. The resulting λ of H_2I-*R*-3*m* is 0.59 at 260 GPa; the ω_{log} calculated from the phonon spectrum is 1384.5 K. The superconducting critical temperature T_c was estimated by using the Allen-Dynes-modified McMillan equation[39] $T_C = \frac{\omega_{log}}{1.2}\exp\left[\frac{1.04(1+\lambda)}{\lambda-\mu^*(1+0.62\lambda)}\right]$. Using the Coulomb pseudopotential μ^* of 0.1 and 0.13, the T_c for H_2I-*R*-3*m* are obtained in the range of 21.6 K to 30.8 K at 260 GPa. Similarly, the calculated T_c for H_2I-*Pnma* at 100 GPa and H_4I-*P*6/*mmm* at 120 GPa reaches 5.3 K and 9.9 K, respectively. Furthermore, the T_c for the three structures as a function of pressure are calculated, as listed in Table I. The results show that for H_2I-*R*-3*m*, T_c decreases with increasing pressure. While for H_2I-*Pnma* and H_4I-*P*6/*mmm*, T_c first decrease and then increase as pressure increasing.

To study the underlying superconducting mechanism, the Eliashberg spectral function $\alpha^2F(\omega)$ and integrated λ for H_2I-*Pnma*, H_2I-*R*-3*m* and H_4I-*P*6/*mmm* phases are presented in Fig. 6. The absence of any imaginary frequency indicates their dynamical stability. Three separate regions of phonon bands are clearly recognized, which are also suitable for the other H-rich compounds. The low-frequency bands come mainly from the lattice vibrations of the heavy I atom, the intermediate-frequency region are due to H–I–H bending and H-I wagging vibrations, high-frequency are mostly related to the H_2 molecular stretching modes.

For H_2I-*R*-3*m* phase, low-frequency I vibrations (below 12 THz) contribute approximately 22.7% in total λ, whereas the intermediate-frequency (31-55 THz) contribute 77.3% of λ. Note that there is no high-frequency vibration because H_2 molecular units disappear. This result highlights that H-derived bending and wagging modes play a significant role in superconductivity. The physical mechanism is similar to those in H_3S (*Im*-3*m*) and CaH_6 (*Im*-3*m*), where intermediate-frequency vibrations dominate the superconductivity. These materials have

the same characteristics that they all possess atomic phase with high T_c. For H_2I-*Pnma* phase, the low-frequency I vibrations (< 9 THz), intermediary-frequency (16-38 THz) and high-frequency H_2 units frequency (> 91 THz) contribute 54.6%, 39.8%, and 5.6% to the EPC, respectively. And for H_4I-*P*6/*mmm* phase, the low-frequency, intermediary-frequency and high-frequency provide a contribution 34.9%, 55.7%, and 9.4% of the total λ, respectively. It is found that in the H_2I-*Pnma* and H_4I-*P*6/*mmm* containing H_2 molecular units, the intermediary-frequency and low-frequency vibrations are mainly responsible for λ, while the contribution of H_2 vibration is small. The superconductivity mechanism of H_2I-*Pnma* and H_4I-*P*6/*mmm* is similar to that of $SiH_4(H_2)_2$ and $GeH_4(H_2)_2$,[15, 16] where they all have H_2 molecular units.

To further study what can improve the superconductivity, some physical parameters between *Pnma* and *R*-3*m* phases in H_2I at 240 GPa are compared. As mentioned above, *Pnma* phase has H_2 molecular units, while in *R*-3*m* phase H_2 molecular units disappear and form atomic phase. Firstly, DOS values at E_f of *R*-3*m* phase (3.3×10^{-2} states/eV/Å^3) is nearly 1.5 times larger than that of *Pnma* phase (2.3×10^{-2} states/eV/Å^3). Secondly, the values of EPC λ and ω_{log} of *R*-3*m* phase are also 1.5 times as much as that of *Pnma* phase, as shown in Table I. The enhancement of EPC λ, ω_{log}, and DOS values lead to an increase of T_c for *R*-3*m* phase to 33 K which is approximately 8 times larger than that of *Pnma* phase (3.8 K). As a comparison, the *R*-3*m* is alike with other hydrogen-rich compounds, in which the H_2 quasi-molecules have been broken, such as H_3S and CaH_6. While the *Pnma* structure is resemble to high-pressure structures of $SiH_4(H_2)_2$ and $GeH_4(H_2)_2$, where they posses H_2 molecular units. Although the T_c of $SiH_4(H_2)_2$ (107 K) and $GeH_4(H_2)_2$ (90 K) are high, they still smaller than the atomic phase of H_3S (200 K) and CaH_6 (235 K). We think that if the H_2 molecular in these hydrogen-rich systems are broken, the superconducting transition temperature T_c will be increased by several times.

CONCLUSION

In summary, the structures, stability, metallization, and superconductivity of iodine hydrides at high pressures are investigated by *ab initio* calculations. Three stoichiometries of H_2I, H_4I and H_5I are uncovered at high pressures. H_2I with *Pnma* symmetry is stable above 100 GPa which contains H_2 molecule units. Interestingly, H_2 molecules units are broken and form a novel atomic phase with *R*-3*m* symmetry at 246 GPa. Electron-phonon coupling calculations show that the T_c of *Pnma* and *R*-3*m* phases are 3.8 K and 33 K at 240 GPa, respectively. Significantly, the T_c of atomic phase *R*-3*m* is raised 8 times than that of *Pnma*, because the physical parameters of EPC λ, ω_{log}, and DOS values at E_f related with T_c are enhancement in atomic phase *R*-3*m*.

AUTHOR INFORMATION

Corresponding Author, *E-mail: cuitian@jlu.edu.cn

ACKNOWLEDGMENT

This work was supported by the National Basic Research Program of China (No. 2011CB808200), National Natural Science Foundation of China (Nos. 11204100, 51572108, , 11574109, 11404134, 11504127), Program for Changjiang Scholars and Innovative Research Team in University (No. IRT1132), National Found for Fostering Talents of basic Science (No. J1103202). China Postdoctoral Science Foundation (2012M511326, 2013T60314, and 2014M561279). Part of calculations were performed in the High Performance Computing Center (HPCC) of Jilin University.

REFERENCES

1. E. Wigner and H. B. Huntington, *J. Chem. Phys.*, 1935, **3**, 764-770.
2. N. W. Ashcroft, *Phys. Rev. Lett.*, 1968, **21**, 1748.
3. C. J. Pickard and R. J. Needs, *Nat. Phys.*, 2007, **3**, 473-476.
4. H. Liu, H. Wang and Y. Ma, *J. Phys. Chem. C*, 2012, **116**, 9221-9226.
5. J. M. McMahon and D. M. Ceperley, *Phys. Rev. B*, 2011, **84**, 144515.
6. M. I. Eremets and I. A. Troyan, *Nat. Mater.*, 2011, **10**, 927-931.
7. C.-S. Zha, Z. Liu and R. J. Hemley, *Phys. Rev. Lett.*, 2012, **108**, 146402.
8. N. W. Ashcroft, *Phys. Rev. Lett.*, 2004, **92**, 187002.
9. X.-J. Chen, J.-L. Wang, V. V. Struzhkin, H.-k. Mao, R. J. Hemley and H.-Q. Lin, *Phys. Rev. Lett.*, 2008, **101**, 077002.
10. M. Martinez-Canales, A. R. Oganov, Y. Ma, Y. Yan, A. O. Lyakhov and A. Bergara, *Phys. Rev. Lett.*, 2009, **102**, 087005-087004.
11. G. Gao, A. R. Oganov, A. Bergara, M. Martinez-Canales, T. Cui, T. Iitaka, Y. Ma and G. Zou, *Phys. Rev. Lett.*, 2008, **101**, 107002-107004.
12. J. S. Tse, Y. Yao and K. Tanaka, *Phys. Rev. Lett.*, 2007, **98**, 117004-117004.
13. G. Gao, A. R. Oganov, P. Li, Z. Li, H. Wang, T. Cui, Y. Ma, A. Bergara, A. O. Lyakhov, T. Iitaka and G. Zou, *Proc. Natl Acad. Sci. USA*, 2010, **107**, 1317-1320.
14. X. Jin, X. Meng, Z. He, Y. Ma, B. Liu, T. Cui, G. Zou and H.-k. Mao, *Proc. Natl Acad. Sci. USA*, 2010, **107**, 9969-9973.
15. Y. Li, G. Gao, Y. Xie, Y. Ma, T. Cui and G. Zou, *Proc. Natl. Acad. Sci. USA*, 2010, **107**, 15708-15711.

16. G. Zhong, C. Zhang, X. Chen, Y. Li, R. Zhang and H. Lin, *J. Phys. Chem. C*, 2012, **116**, 5225-5234.
17. Y. Xie, Q. Li, A. R. Oganov and H. Wang, *Acta Crystallogr., Sect. C*, 2014, **70**, 104-111.
18. D. Zhou, X. Jin, X. Meng, G. Bao, Y. Ma, B. Liu and T. Cui, *Phys. Rev. B*, 2012, **86**, 014118.
19. H. Wang, J. S. Tse, K. Tanaka, T. Iitaka and Y. Ma, *Proc. Natl. Acad. Sci. USA*, 2012, **109**, 6463-6466.
20. D. Duan, Y. Liu, F. Tian, D. Li, X. Huang, Z. Zhao, H. Yu, B. Liu, W. Tian and T. Cui, *Sci. Rep.*, 2014, **4**, 6968.
21. D. Duan, X. Huang, F. Tian, D. Li, H. Yu, Y. Liu, Y. Ma, B. Liu and T. Cui, *Phys. Rev. B*, 2015, **91**, 180502.
22. A. P. Drozdov, M. I. Eremets, I. A. Troyan, V. Ksenofontov and S. I. Shylin, *Nature*, 2015, **525**, 73-76.
23. A. Ikram, B. H. Torrie and B. M. Powell, *Mol. Phys.*, 1993, **79**, 1037 - 1049.
24. J. van Straaten and I. F. Silvera, *Phys. Rev. Lett.*, 1986, **57**, 766.
25. J. van Straaten and I. F. Silvera, *Phys. Rev. B*, 1987, **36**, 9253.
26. A. Shamp and E. Zurek, *J. Phys. Chem. Lett.*, 2015, DOI: 10.1021/acs.jpclett.5b01839, 4067-4072.
27. Y. Wang, J. Lv, L. Zhu and Y. Ma, *Phys. Rev. B*, 2010, **82**, 094116.
28. Y. Wang, J. Lv, L. Zhu and Y. Ma, *Comput. Phys. Commun.*, 2012, **183**, 2063-2070.
29. G. Kresse and D. Joubert, *Phys. Rev. B*, 1999, **59**, 1758-1775.
30. G. Kresse and J. Furthmüller, *Phys. Rev. B*, 1996, **54**, 11169-11186.
31. J. P. Perdew, K. Burke and M. Ernzerhof, *Phys. Rev. Lett.*, 1996, **77**, 3865-3868.
32. G. Paolo, B. Stefano, B. Nicola, C. Matteo, C. Roberto, C. Carlo, C. Davide, L. C. Guido, C. Matteo, D. Ismaila, C. Andrea Dal, G. Stefano de, F. Stefano, F. Guido, G. Ralph, G. Uwe, G. Christos, K. Anton, L. Michele, M.-S. Layla, M. Nicola, M. Francesco, M. Riccardo, P. Stefano, P. Alfredo, P. Lorenzo, S. Carlo, S. Sandro, S. Gabriele, P. S. Ari, S. Alexander, U. Paolo and M. W. Renata, *J. Phys.: Condens. Matter*, 2009, **21**, 395502.
33. A. V. Krukau, O. A. Vydrov, A. F. Izmaylov and G. E. Scuseria, *J. Chem. Phys.*, 2006, **125**, 224106.
34. J. Heyd, G. E. Scuseria and M. Ernzerhof, *J. Chem. Phys.*, 2003, **118**, 8207-8215.
35. M. D. Segall, P. J. D. Lindan, M. J. Probert, C. J. Pickard, P. J. Hasnip, S. J. Clark and M. C. Payne, *J. Phys.: Condens. Matter*, 2002, **14**, 2717-2744.
36. O. Shimomura, K. Takemura, Y. Fujii, S. Minomura, M. Mori, Y. Noda and Y. Yamada, *Phys. Rev. B*, 1978, **18**, 715.
37. Y. Fujii, K. Hase, N. Hamaya, Y. Ohishi, A. Onodera, O. Shimomura and K. Takemura, *Phys. Rev. Lett.*, 1987, **58**, 796.
38. D. Duan, X. Jin, Y. Ma, T. Cui, B. Liu and G. Zou, *Phys. Rev. B*, 2009, **79**, 064518-064517.
39. P. B. Allen and R. C. Dynes, *Phys. Rev. B*, 1975, **12**, 905-922.

Captions of figure

Fig. 1 (a), Formation enthalpies of H-I system with respect to decomposition into constituent elemental solids under pressure. Dashed lines connect data points, and solid lines denote the convex hull. (b), Predicted pressure-composition phase diagram of H-I system

Fig. 2 Structures of stable stoichiometries in H-I system. **(**a) H_2I-*Cmcm*. (b) H_2I -*R*-3*m*. (c) H_4I-*P6*/*mmm*. (d) H_5I-*P*222_1. Purple and pink spheres represent I and H atoms, respectively.

Fig. 3 (a) Calculated enthalpy differences of *Cmcm*, *P*1, *Pnma*, and *R*-3*m* phases in H_2I relative to *Cmcm* phase as a function of pressure. (b) The nearest neighbor distances of H-H, H-I, and I-I in H_2I as a function of pressure.

Fig. 4 The calculated ELF of (a) H_2I-*Pnma* for (010) plane, (b) H_2I-*R*-3*m* for (110) plane, (c) H_2I-*R*-3*m* with isosurface value of 0.7, (d) H_4I-*P6*/*mmm* for (001) plane, (e) H_5I-*P*222_1 contain a H-I square, (d) H_5I-*P*222_1 with isosurface value of 0.8.

Fig. 5. Electronic band structure for (a) H_2I-*Pnma* at 100 GPa, (b) H_2I-*R*3*m* at 260 GPa, and (c) H_4I-*P6/mmm* at 120 GPa. The dashedline indicates the Fermi level. (d) The evolution of band gaps of the H_5I-*P*222_1 with increasing pressure.

Fig. 6. Phonon dispersion curves, phonon density of states (PHDOS) projected on I and H atoms, and Eliashberg spectral function $\alpha^2F(\omega)$ together with the electron-phonon integral $\lambda(\omega)$ for (a) H_2I-*Pnma* at 100 GPa, (b) H_2I-*R*3*m* at 260 GPa, and (c) H_4I-*P*6/*mmm* at 120 GPa.

Table I The phonon frequency logarithmic average (ω_{log}), EPC parameter (λ), and critical temperature T_c (μ^*= 0.1 and 0.13) for H_2I and H_4I at different pressures.

Phase	P(GPa)	ω_{log}(K)	λ	T_c(K)μ^*=0.1	T_c(K)μ^*=0.13
H_2I	100	552.6	0.472	5.30	3.00
Pnma	150	729.2	0.427	4.32	2.12
	200	834.6	0.403	3.67	1.62
	240	917.7	0.398	3.77	1.62
H_2I	240	1366.2	0.611	33.05	23.55
R-3*m*	260	1384.5	0.594	30.82	21.57
	300	1465.8	0.548	25.09	16.53
H_4I	120	792.9	0.500	9.92	6.04
*P*6/*mmm*	160	898.5	0.474	8.80	5.01
	200	960.4	0.476	9.57	5.48
	250	981.0	0.493	11.26	6.70
	300	849. 4	0.525	12.48	7.92

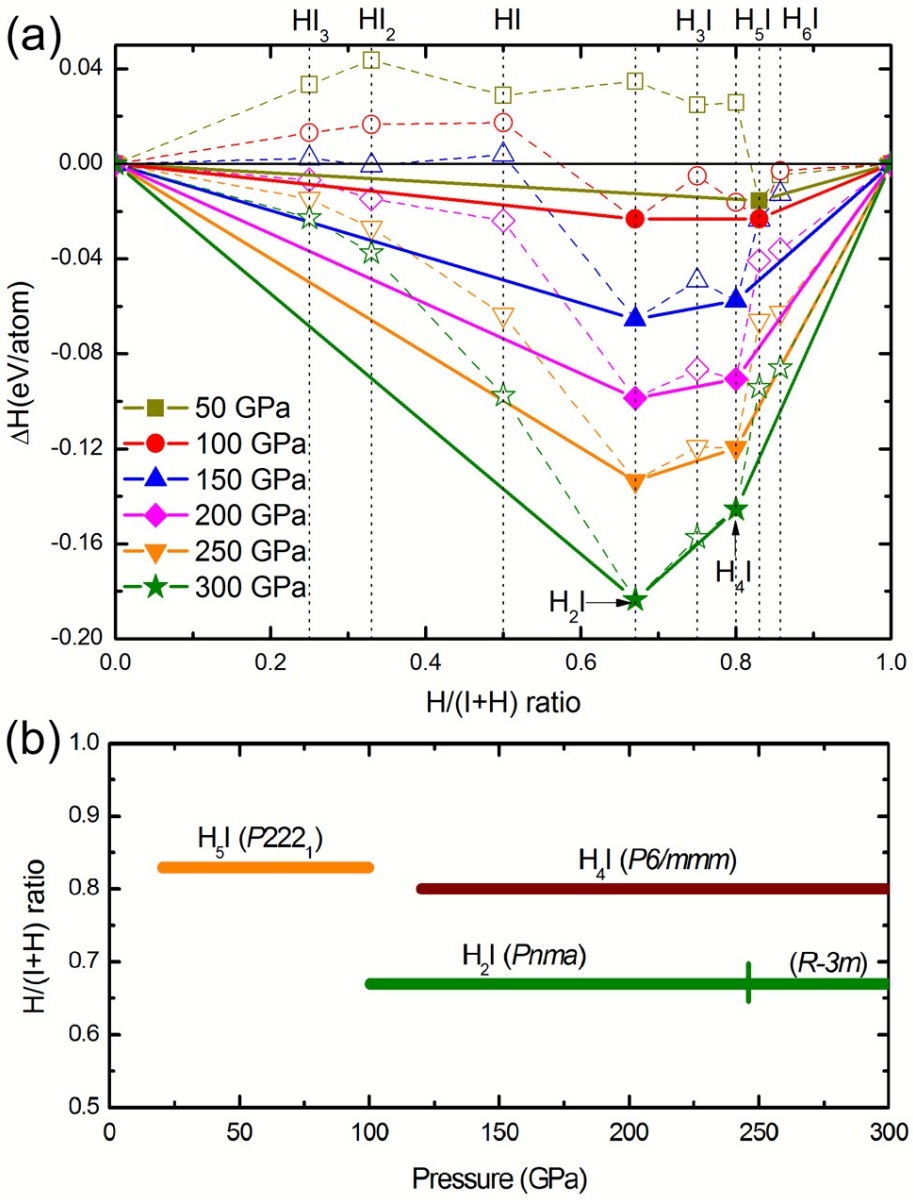

Fig. 1

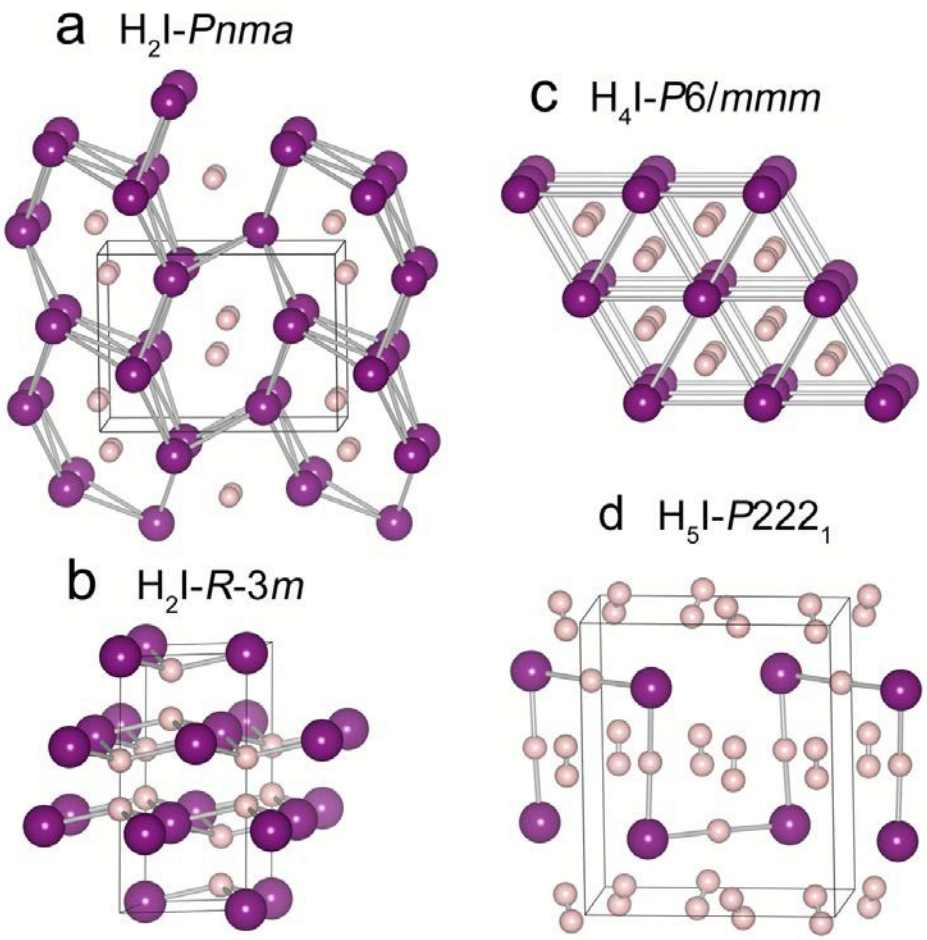

Fig. 2

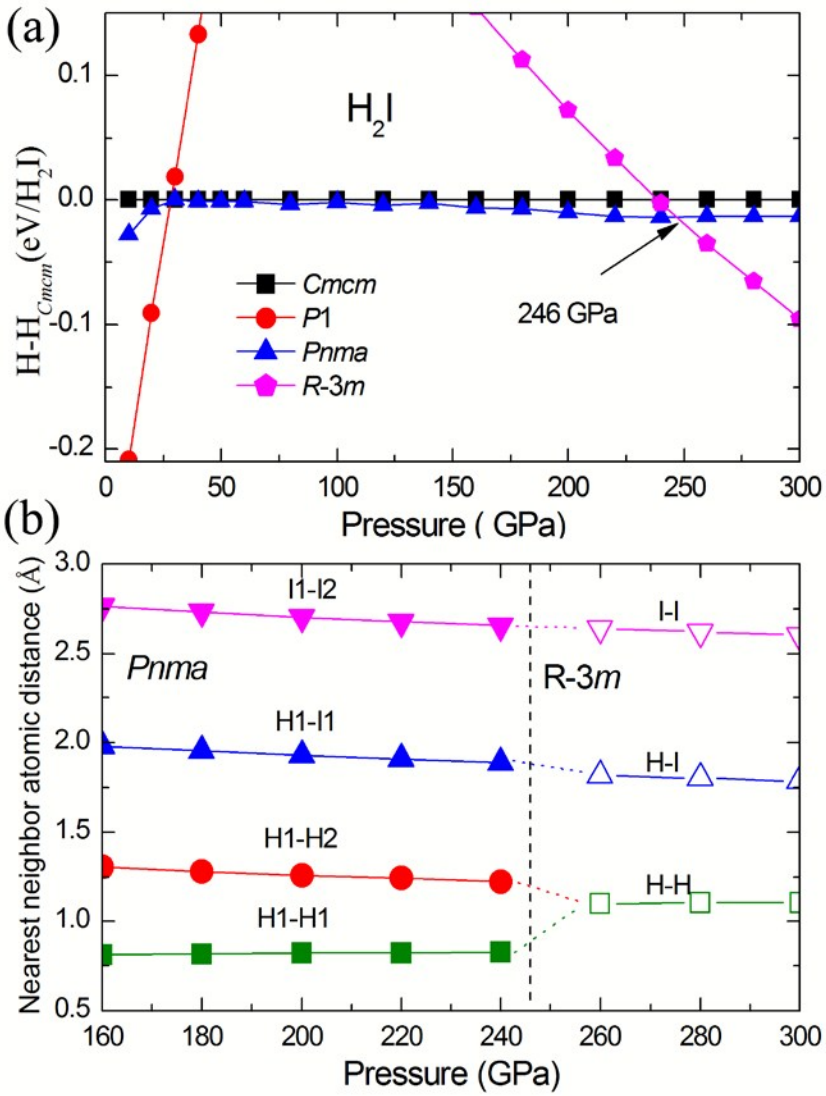

Fig.3

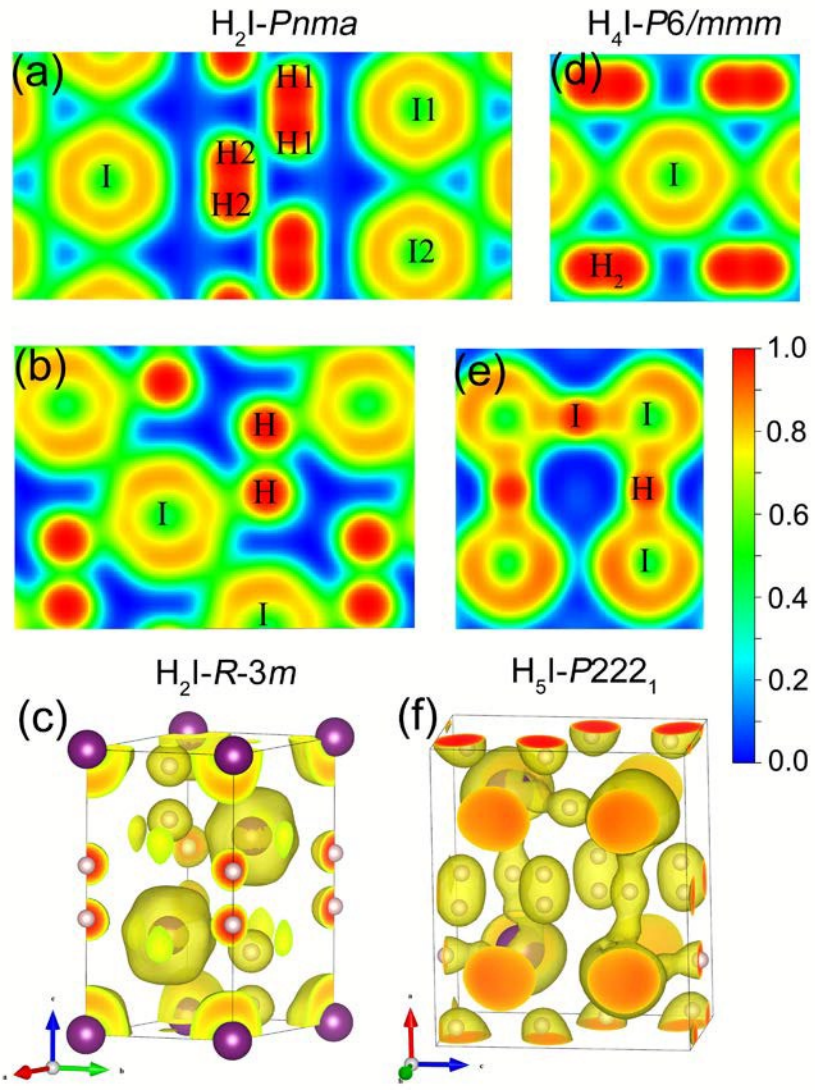

Fig. 4

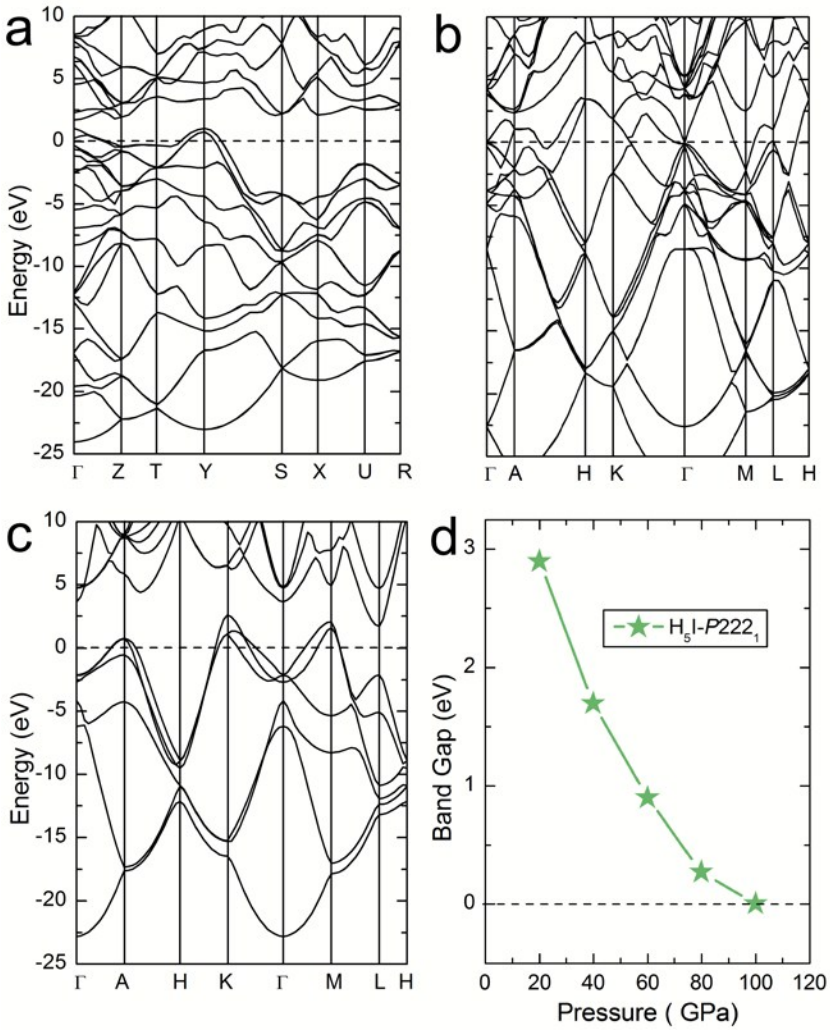

Fig. 5

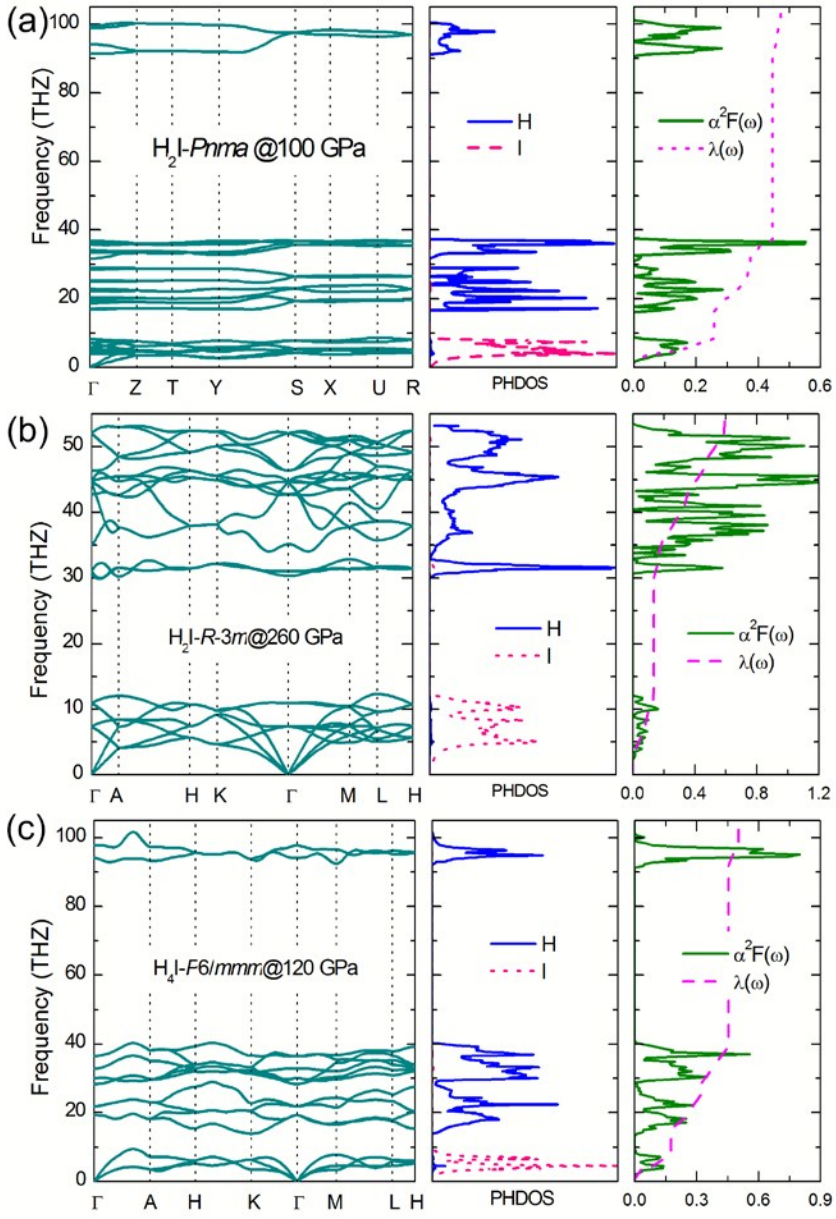

Fig. 6

For Table of Contents Use Only

Enhancement of T_c in atomic phase of iodine-doped hydrogen at high pressures

Defang Duan, Fubo Tian, Yunxian Liu, Xiaoli Huang, Da Li, Hongyu Yu, Yanbin Ma, Bingbing Liu, Tian Cui[*]

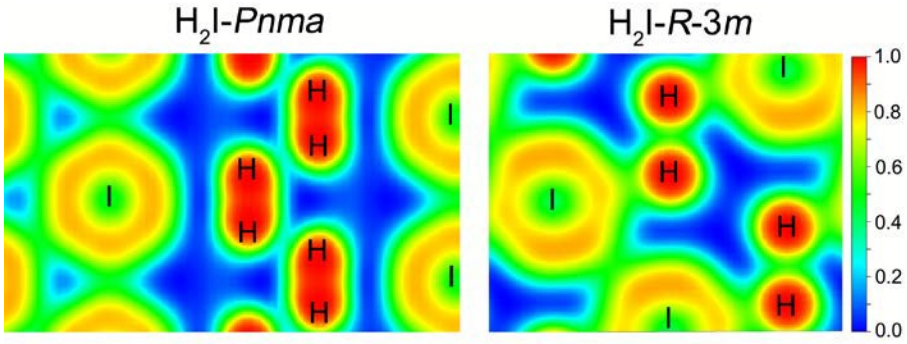

H_2 molecule units dissociate and form a novel atomic phase with *R*-3*m*.

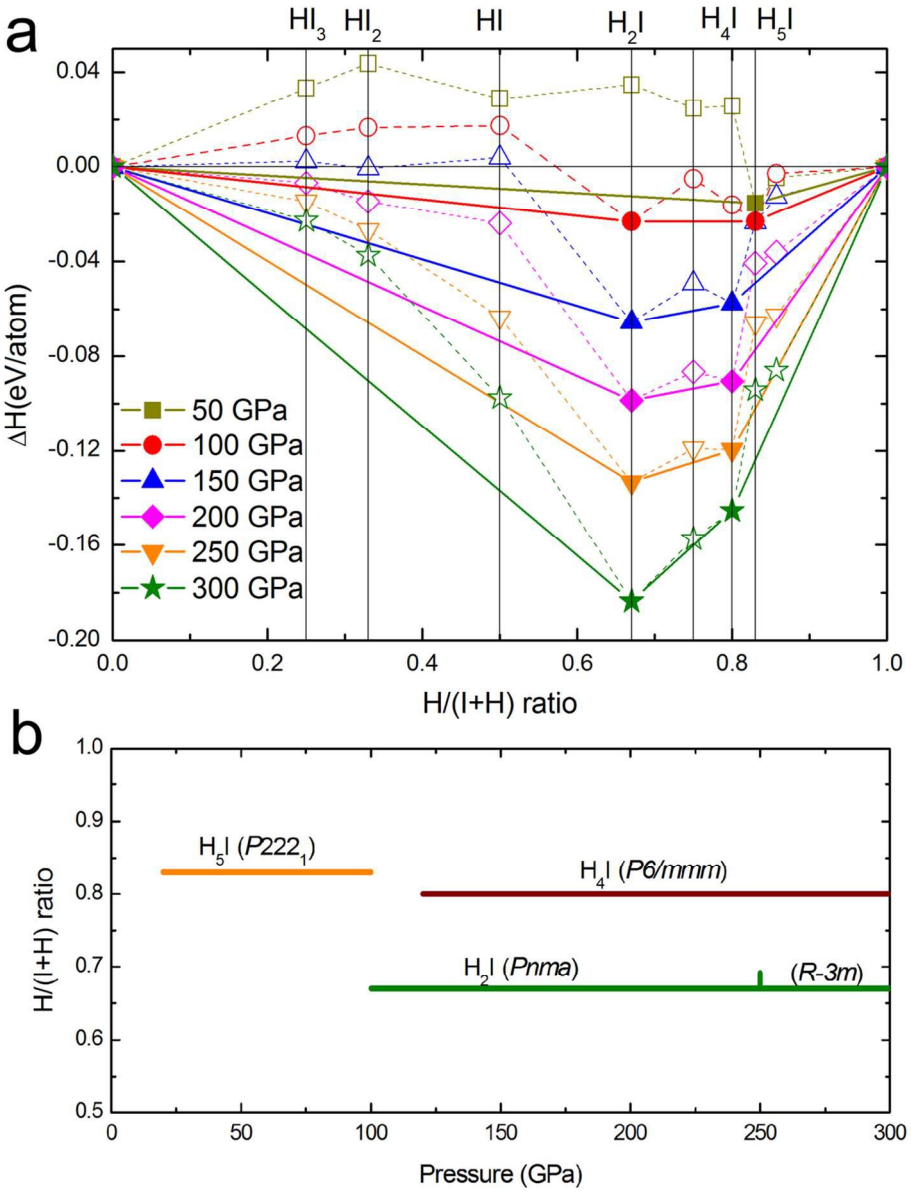

107x141mm (300 x 300 DPI)

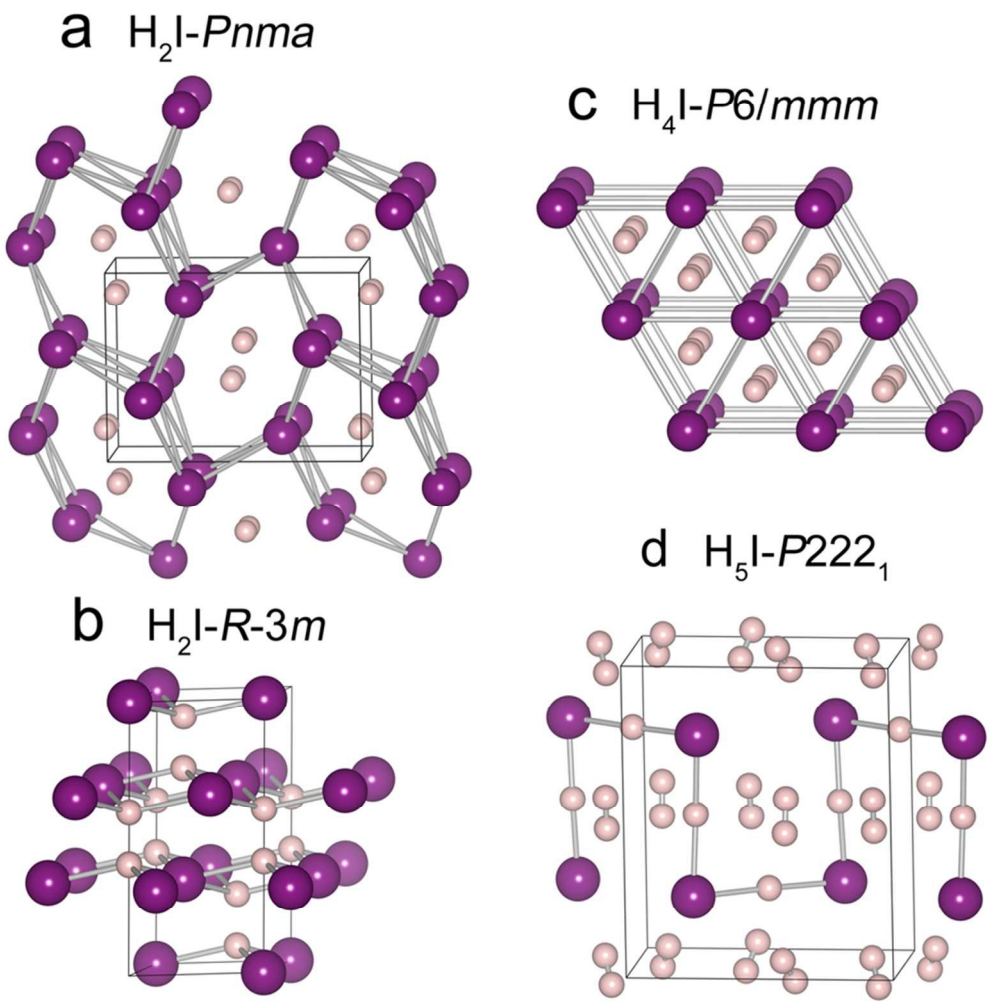

82x82mm (300 x 300 DPI)

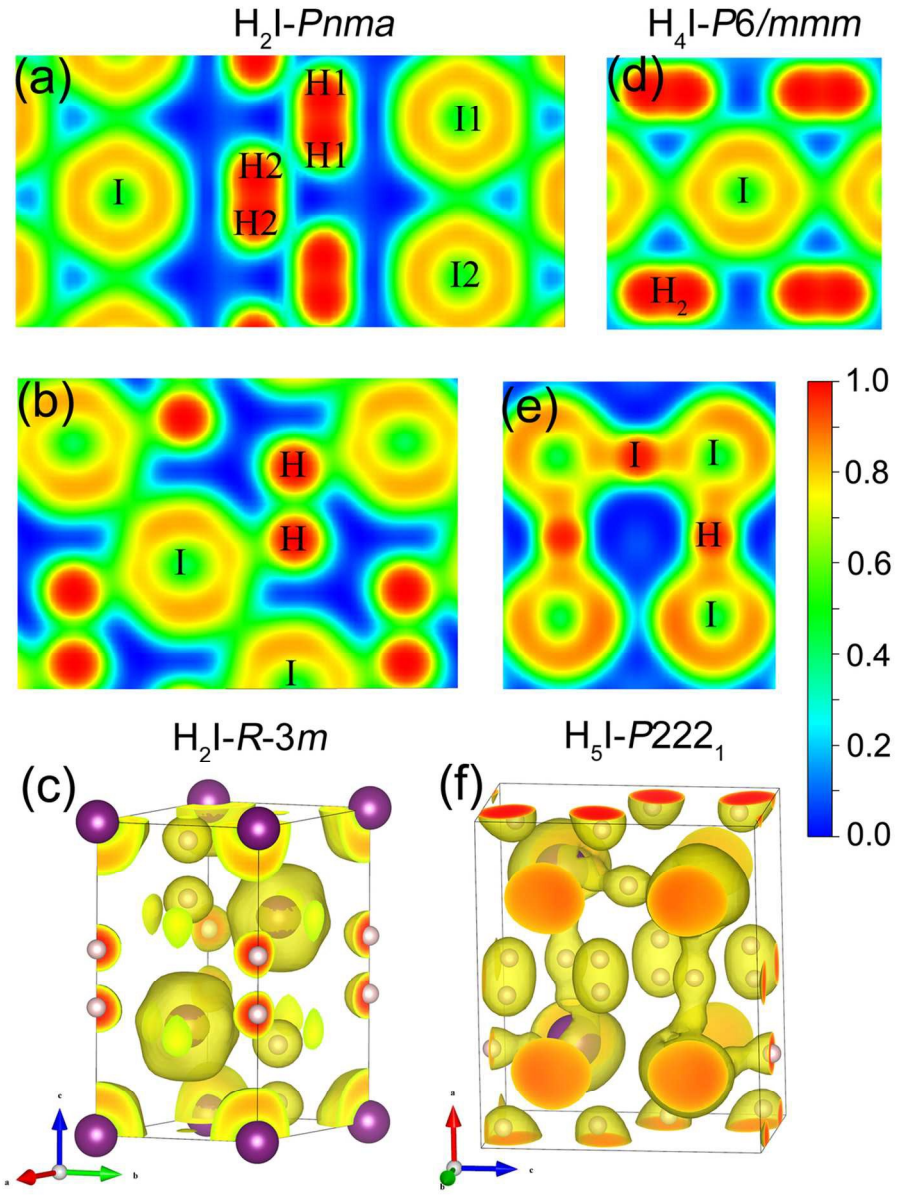

108x142mm (300 x 300 DPI)

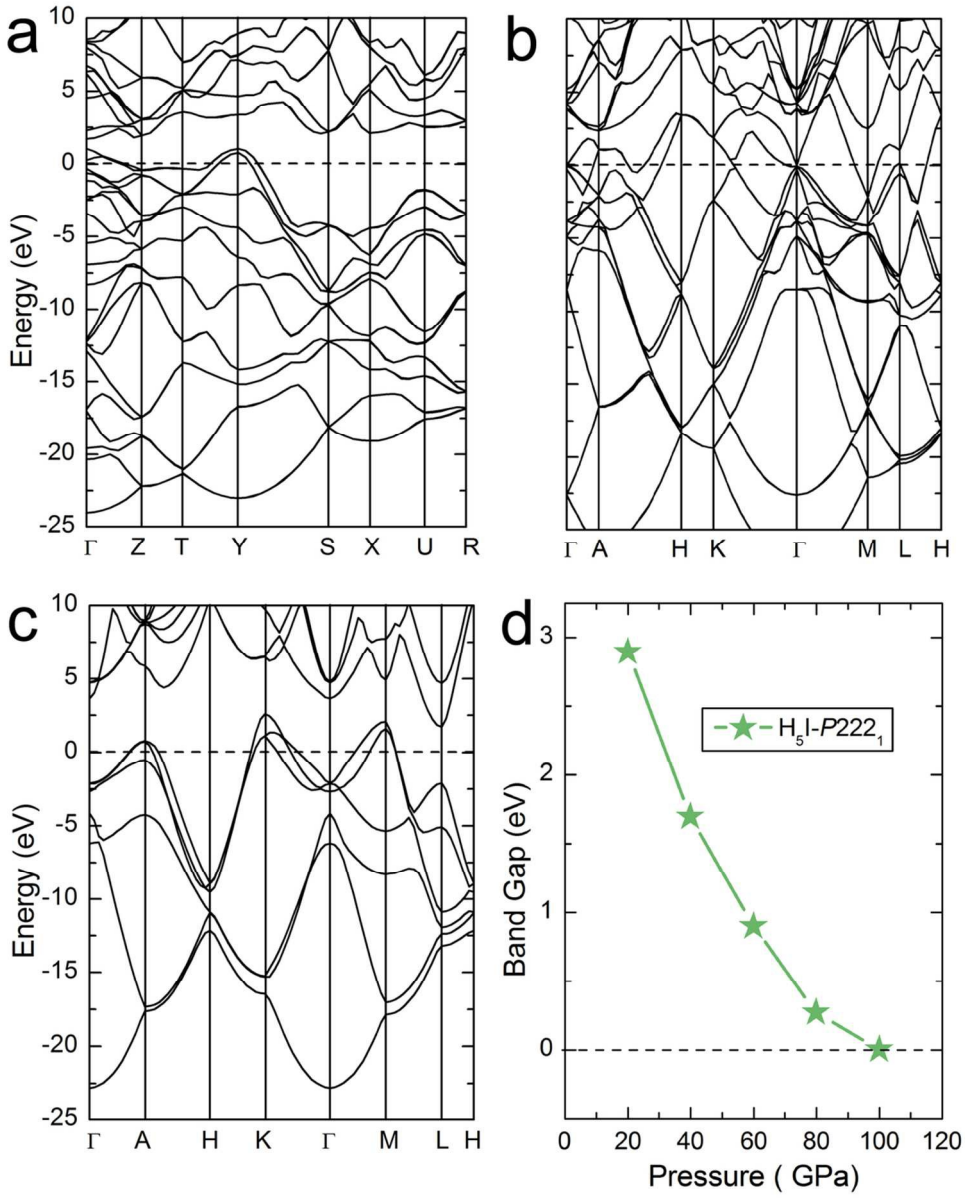

102x127mm (300 x 300 DPI)

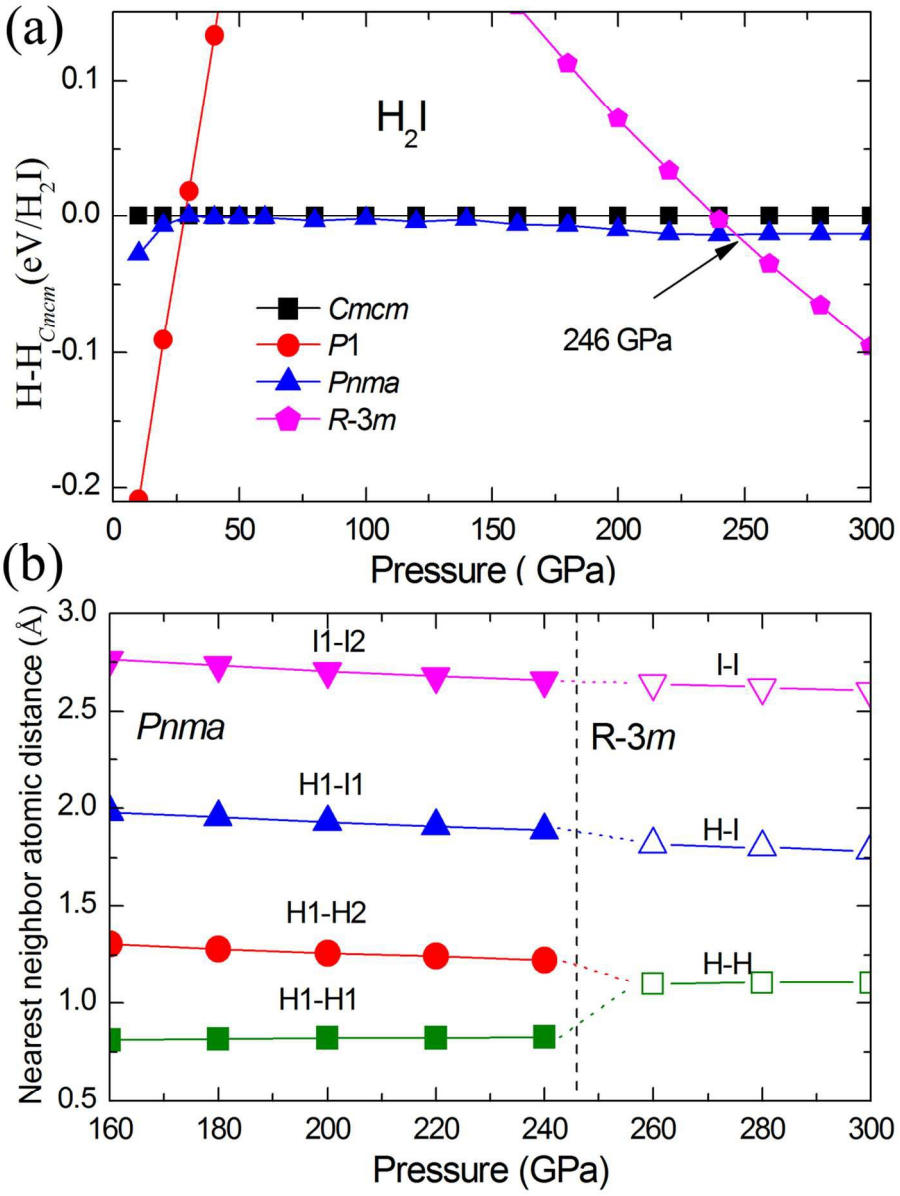

109x145mm (300 x 300 DPI)

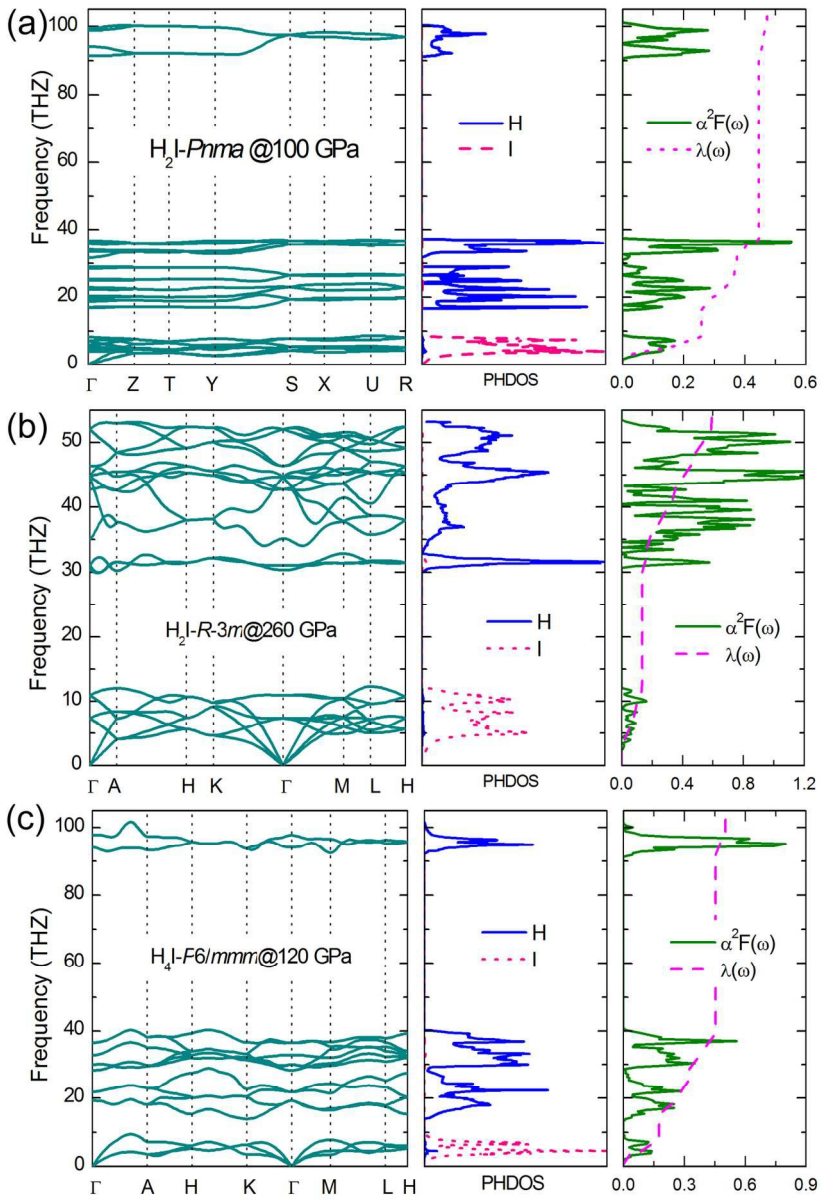

123x180mm (300 x 300 DPI)